This paper has been submitted to the journal of 'Microgravity Science and Technology.' manuscript No.
(will be inserted by the editor)

Prediction and Control of Internal Condensing Flows in the Experimental Context of their Inlet Condition Sensitivities

M. Kivisalu · P. Gorgitrattanagul · S. Mitra · R. Naik · A. Narain

the date of receipt and acceptance should be inserted later

Abstract The reported experimental results involve *fully condensing* flows of pure FC-72 vapor on a horizontal condensing surface (316 stainless steel) which is the bottom surface (wall) of a rectangular cross-section duct of 2 mm height, 15 mm width, and 1 m length. The sides and top of the duct are made of clear plastic. The experimental system in which this condenser is used is able to control steady-in-the-mean (termed quasi-steady) mass flow rate, exit pressure, and wall cooling conditions. It has been found that, with the condenser mean (time averaged) inlet mass flow rate, exit pressure, and wall cooling condition held fixed at steady values, there is a very strong sensitivity to high amplitude pressure fluctuations and flow rate pulsations at the condenser inlet. This sensitivity often significantly alters the condenser mean inlet pressure, pressure drop, local heat transfer rates ($>$ 200% increase at certain locations), and the condensing flow morphology. These effects are representative of fluctuations / pulsations that are typically encountered in applications but are either not accounted for or are not detected. The effects of imposed fluctuations / pulsations, as opposed to cases involving negligible imposed fluctuations / pulsations, are dependent on the amplitude and the frequency content of the imposed fluctuations and this is discussed in a separate paper. A significant upstream annular regime portion of the reported shear / pressure driven fully condensing flows operate under conditions where the laboratorys transverse gravity effects are negligible and, therefore, the identified sensitivity phenomenon is highly relevant to zero- or micro-gravity conditions. The micro-gravity relevance of this sensitivity for the annular regime phenomenon is currently also being demonstrated with the help of computations and simulations.

Department of Mechanical Engineering - Engineering Mechanics Michigan Technological University, Houghton, MI 49931 E-mail: narain@mtu.edu

Keywords horizontal channel condensation · fluctuation sensitivity · internal condensing flows · flow pulsation

1 Introduction

This paper presents a fundamental experimental investigation of a pressure / shear driven internal condensing flow's quasi-steady pressure-difference sensitivity to the amplitude and frequency of pressure fluctuations (or flow rate pulsations) at the inlet of the condenser. Inadvertently or deliberately, such imposed pressure-difference fluctuations frequently occur in closed flow loops in which the condensing flow is primarily shear driven and devices like turbines or reciprocating compressors introduce significant pressure pulsations to the vapor supplied to the condenser. For the fluctuation case reported here, pressure pulsation amplitude on the order of 750 Pa (on a mean inlet pressure of about 140 kPa) and frequency 9.8 Hz induces large pulsations in the inlet mass flow rates and changes the quasi-steady flow. This is because the pressure - difference across the frontal annular portion of the flow is itself small - of the order of 500 Pa - and comparable to imposed fluctuations and the pressure - difference across the entire condenser is also small (of the order of 1 kPa). Full data matrix covering a range of amplitudes and frequencies is reported elsewhere in Kivisalu et al., 2011. The experimental results reported here are important to a meaningful assessment of a shear driven condenser's performance in any closed flow loop facility - be it an experimental facility or a system of practical interest. Shear / pressure driven internal condensing flows are of interest here because they occur in horizontal ducts, micro-gravity, and micro-meter scale hydraulic diameter ducts of interest for next generation space based thermal management systems and high heat-flux electronic cooling applications.

For assistance in the development of predictive abilities for condensing flows, there are many experimental papers that deal with condensation of pure vapors flowing inside vertical or horizontal ducts (of circular or rectangular cross-sections, as in Goodykoontz and Dorsch 1966, Cavallini and Zechchin 1971, etc.). The experiments as well as related correlations (Shah 1979, Cavallini et al. 1974, etc.) in the literature cover a large set of flow regimes and associated flow physics categories (see Mitra et al. 2011 and Kurita et al. 2011).

The new experimental results reported here complement and improve the experimental results reported in the computational work of Kulkarni et al. 2011 that attempt to show that shear / pressure driven flows, as compared to gravity driven flows, need very different specifications and control for inlet / exit conditions. Furthermore, as shown in Kurita et al. (2011), gravity driven condensing flow experiments do not show significant sensitivity to the presence of reported levels of the inlet pressure fluctuations. Also, we have experimentally confirmed - for shear driven condensing flows - the result that, in the case of negligible amplitude imposed inlet flow rate / pressure - difference fluctuations, the mean pressure - difference across the condenser is well defined, and no other pressure - difference can be imposed for the same specified and steady mean inlet (or exit) pressure, mean inlet mass flow rate, and mean cooling conditions. However, shear / pressure driven fully condensing flows quasi-steady realizations under quasi-steady prescriptions are not repeatable unless the mean boundary conditions are specified along with relevant information on the level of superposed / imposed fluctuations. For example, for the experiments described in this paper, prescripitions of mean inlet flow rate, one of the mean boundary pressures (exit or inlet), and cooling conditions for the condensing - surface are not sufficient, by themselves, to ensure the flows' repeatability. The additional information on the content of amplitude and frequencies present in the superposed fluctuations are necessary to make theses flows deterministic and repeatalble.

The reported results advance prediction and control capabilities for shear / pressure driven internal condensing flows (in micro - gravity or micro - scale ducts) in the context of their unique sensitivities to inadvertent or deliberate impositions of fluctuations / pulsations on the mean values of pressure - difference or flow rate.

The sensitivity reported here for fully condensing flows is also useful in understanding the variety of complex flow morphologies (Wu and Cheng (2005) & Coleman and Garimella (2003)) and transient phenomena (Wedekind and Bhatt 2010, etc.) that are possible for shear / pressure driven flow condensation. A similar result is expected to hold for flow boiling, and our group is currently establishing this experimentally. These sensitivities for flow boiling will be helpful

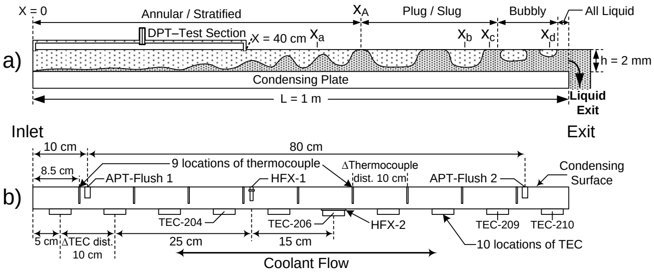

Fig. 1 Side views of: (a) test-section, and (b) instrumented condensing plate

in understanding flow transients and instabilities (Brutin et al. 2003, Kandlikar 2002, etc.) that are known to be present for shear / pressure driven micro-scale flow boiling.

New computational results in support of the reported / expected experimental results for unsteady and quasi-steady shear / pressure driven condensing flows - both for micro-gravity as well as horizontal channel experiment - will be reported in the near future. In conclusion, by giving proper attention to the newly identified sensitivities in the planning and design of new shear / pressure driven flow experiments and associated devices, one should be able to achieve both repeatable and predictable condenser (or boiler) performance in space, small to micro-scale diameter tubes, etc.

Nomenclature

$\bar{T}_w$ — mean wall temperature of condenser

Δp — pressure difference across the condenser length unless subscripts indicate otherwise (kPa)

$\dot{M}_{in}$ — mass flow rate of vapor supplied to condenser (g/s)

h_{fg} — enthalpy of vaporization for the condenser working fluid in condenser (kJ/kg)

p — pressure (kPa)

p^*_{exit} — exit pressure feedback control set point (kPa)

PID — proportional-integral-derivative (of feedback control)

t — time (seconds or minutes)

T_{bath} — temperature of water surrounding evaporator in Fig. 2 (deg C)

TEC — thermo electric cooler (solid state electronic heat pump)

x — distance from condenser inlet in direction of flow (cm)

x_A — length of annular flow regime in condenser (cm), see Fig. 1a

Subscript	Description
in	at condenser inlet
exit	at condenser exit
N-F	associated with a no-fluctuation imposed case for condensing flows
I-F	associated with an imposed-fluctuation condensing flow case

2 Experimental Set-up

2.1 Description

Fully condensing flows of FC-72 vapor in a horizontal rectangular cross-section (2 mm gap height and 15 mm wide) duct of 1 m length, as shown in Fig. 1, are investigated. Its horizontal condensing surface area (15 mm x 1 m) is the top of a 12.7 mm thick stainless steel plate. The top and side surfaces of the channel are made of a thick transparent material (lexan), which is covered with an insulation that can be removed to allow flow visualization.

Transport and thermodynamic fluid properties of FC-72 are available from 3M Corporation. This choice of fluid is for safety of operations under laboratory conditions at a university. Prediction for other fluids is to be made available with the help of computations and planned new experiments with water.

The flow-loop in Fig. 2 has three independent feedback control strategies that can fix steady-in-the-mean values of: inlet mass flow rate $\bar{\dot{M}}_{in}$, condensing-surface cooling conditions, and exit pressure $\bar{p}_{exit}$. Mean inlet mass flow rate $\bar{\dot{M}}_{in}$ is fixed through active feedback control of the power input to the electric heater inside the evaporator / boiler. Evaporator pressure is stabilized using the surrounding water reservoir temperature. Condensing-surface temperature $T_W(x)$ is obtained for a fully specified steady cooling approach that results from a specified water flow rate and temperature (at the location where the flowing coolant water first approaches the condenser plate). The cooling approach may further be specified depending on whether or not additional and specified cooling conditions from feedback controlled thermo-electric coolers (TECs) - which are on the bottom surface of the condensing-plate (Fig. 1b) and reject heat into the cooling flow of water - are used. Exit pressure is controlled through active feedback control of the controllable displacement pump P. For some experimental runs, fixing of different mean inlet pressure $\bar{p}_{in}$ values are attempted through manual control of the rpm of the muffled compressor C (which has negligible pressure fluctuations at its exit) - with or without assistance from manual adjustment of the valve V_{BP} and / or the use of the pressure pulsator (described later).

The vapor mass flow rate out of the evaporator, $\dot{M}_{in}$, goes into the test section and is measured by a Coriolis flow meter F_c. This F_c value is controlled, as needed, by a feedback controlled heating of the evaporator. Downstream of the evaporator, in the indicated bypass loop, there is an oil-free, semi-hermetically sealed compressor (which is a positive displacement vane type compressor) which is magnetically coupled to an rpm controlled motor. The purpose of the compressor is to test whether changes in compressor rpm (and / or changing the opening in the valve V_{BP} in the bypass loop) can be used to change the mean test-section inlet pressure while holding the test-section exit pressure approximately fixed. If this is not possible, changes in pressure-difference across the compressor will only change the boiler / evaporator pressure if the mean inlet vapor mass flow rate is eventually brought to the fixed steady value. The sealed enclosure for the compressor is such that it effectively removes all 0-50 Hz frequencies (this is the frequency range of interest for investigating the condenser response) in the pressure fluctuations downstream of the compressor. Since changes in the test-section pressure-difference may be enabled (see Kulkarni et al. 2011) by the amplitude and frequency content of the superposed time-periodic pressure fluctuations at the inlet of the test-section, a pressure pulsator is located downstream of F_c in Fig. 2. This pulsator (a frequency controlled diaphragm compressor, which is used after removing the valves between its suction and compression chambers) cannot change the mean flow rate but is able to provide an independent control on pressure and mass flow rate fluctuations present at the test-section inlet, with frequency being controlled by the pulsator speed and amplitude being controlled by valve V_P.

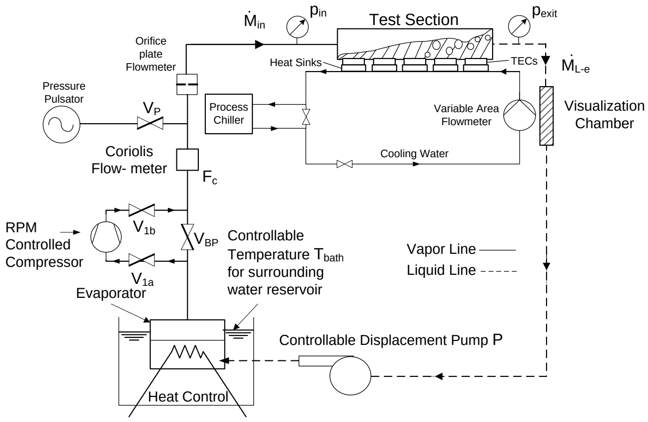

Fig. 2 Schematic of the experimental flow loop

The flow of coolant water in Fig. 2 (also see Kurita et al. 2011) is supplied with the help of a commercially available process chiller and a manually adjusted value of the water flow rate (0 17 liters/min). In addition, as shown in Fig. 1b, various TECs are located in the condensing plate. Each of the TECs can be separately activated and controlled for any additional cooling need.

2.2 Instrumentation

Kulite flush-type absolute pressure-transducers are used in the test-section at locations 10 and 90 cm downstream of the inlet of the test section. Their accuracies, after calibration, are $\pm$ 0.7 kPa. A total of four high accuracy pressure transducers from Omega Engineering are used to measure upstream and downstream absolute pressures for the orifice meter and the condenser. Their accuracies, after calibration, are $\pm$ 0.2 kPa for the test-section transducers and $\pm$ 0.5 kPa for the orifice meter transducers. The accuracies of the other pressure transducers in the system are approximately $\pm$ 0.6 kPa. The variable-reluctance type differential pressure transducer used for the test-section, across locations shown in Fig. 1a, is from Validyne Inc. (it has a post calibration accuracy of $\pm$ 20 Pa). Temperatures are measured by T-type thermocouples with accuracies, after calibration, lying within $\pm$ 1 ^oC. The heat-flux meter HFX-1 (from Vatell Corporation) in Fig. 1b has an accuracy of approximately $\pm$7.2% of its reading, in W/cm^2, and an approximate range of 0-10 W/cm^2 when used with our existing amplifier and data acquisition system. The mean mass flow rate measured from the Coriolis Meter F_c in Fig. 2 is accurate up to $\pm$0.35% of flow, or within $\pm$ 0.007 g/s for the ranges of flow rate (0-2 g/s) investigated here. The orifice plate meter in Fig. 2 is our own design and its dynamic pressure-difference signal in conjunction with computational fluid dynamic analysis yields approximate estimates (see Ajotikar 2011) of the time-varying fluctuating mass flow rates.

For reporting mean quasi-steady data of all variables over minutes to hours, the National Instruments' (NI) data acquisition systems records them at 1 s intervals. The same variables' dynamic data are acquired every 0.5 ms over occasional 5 s intervals. Together, the two rates of data acquisitions reliably yield the signals' frequency content over 0-1000 Hz. The data acquisition devices used to acquire data at 1 s intervals and run the feedback controls are from National Instruments (see Kivisalu et al., 2011 for additional details).

2.3 Cooling Conditions

The condensing surface's cooling approach (which defines its thermal boundary condition) consists of:

- Coolant water flows through heat sinks under the 12.7 mm thick condensing plate at a controlled steady flow rate (1.02 m^3/ hr) and a controlled inlet temperature (15 - 16 ^oC).
- Two thermo-electric coolers (see Fig. 1b), namely TEC-204 and TEC-206, respectively remove heat from the effective area over 30 cm $\leq x \leq$ 40 cm and the effective area over 50 cm $\leq x \leq$ 60 cm. With the help of PID control and thermocouples at x = 38.5 cm and x = 58.5 cm, the temperatures at these locations are respectively held fixed at 40.5 ^oC and 42.5 ^oC.
- The thermo-electric coolers (TEC-209 and TEC-210 in Fig. 1b), removing heat from the approximate region over 80 cm $\leq x \leq$ 1 m, are operated at a fixed driving voltage (14 V) to ensure that the subsequent flow morphology changes rapidly to an all liquid flow by the exit of the test-section.

The above described cooling approaches (with the rest of the TECs being off) define the condensing-surface thermal boundary conditions. These are similar to the ones mathematically defined and modeled in Kulkarni et al. (2011).

2.4 Procedures

2.4.1 No-Fluctuation Steady/Quasi-Steady Flows

The procedure is for achieving steady / quasi-steady fully condensing flows, without fluctuations, whose effective point of full condensation is within the test-section. Downstream of the exit (including the Visualization Chamber in Fig. 2), the flow loop is all liquid up to the evaporator. This procedure involves: (i) keeping the compressor and the pulsator off with the bypass valve (V_{BP} in Fig. 2) fully open, (ii) fixing the evaporator bath temperature T_{bath}, (iii) holding fixed the mean Coriolis mass flow meter F_C (in Fig. 2) reading of the mass flow rate $\bar{M}_{in}$ by a PID control of the evaporator heater, (iv) steadying the condensing surface temperature $T_W(x)$ with the help of the cooling approach described in section 2.3, and (v) using the controllable displacement pump P, through a PID control, to hold the mean exit pressure fixed at $\bar{p}_{exit} = p^*_{exit}$. This procedure allows the inlet pressure p_{in} to freely seek its natural steady value $p_{in}|_{Na}$ to define the natural quasi-steady flow as one with a self-sought pressure-difference $\Delta p|_{Na} = p_{in}|_{Na} - p^*_{exit} \equiv \Delta p|_{N-F}$ for negligible to insignificant pulsator imposed fluctuations (N-F) on vapor flow at the inlet (other inadvertanent and typically small fluctuations are allowed in these N-F cases).

2.4.2 Quasi-Steady Response to Imposed Fluctuations

The following procedure imposes time-varying inlet pressure (and other induced fluctuations) on a quasi-steady flow, while the quasi-steady values of the mass flow rate $\bar{M}_{in}$, exit pressure $\bar{p}_{exit}$, and the steady cooling conditions remain the same as the ones obtained for the original no-imposed fluctuation (N-F) flow. For this procedure, we first achieve a natural (no-fluctuation) quasi-steady flow by the procedure described in section 2.4.1. Using the earlier described flow controls, one continues to hold fixed the values of the mean inlet mass flow rate $\bar{M}_{in}$, mean exit pressure $\bar{p}_{exit} \approx p^*_{exit}$, and other variables that specify the steady cooling conditions described in section 2.3. In addition, the bath temperature T_{bath} surrounding the evaporator is also kept constant. The compressor and / or pulsator speeds are concurrently increased and held at new steady speeds, introducing specific steady-in-the-mean imposed pressure fluctuations (I-F) at the inlet that arise from setting a specific steady driving frequency for the pulsator. If a new quasi-steady mean value of pressure difference, $\Delta\bar{p}\mid_{I-F} \neq \Delta\bar{p}\mid_{N-F}$, is achieved, the new quasi-steady values of the heat flux meter (HFX-1 in Fig. 1b) reading, test-section thermocouple readings, etc. are checked to assess whether a totally new quasi-steady flow compared to the original no-fluctuation (N-F) flow has been achieved. New quasi-steady flow will manifest themselves with altered wall heat-flux, wall temperatures etc, while retaining, approximately, the same overall heat removal rate between the inlet of the condenser and some effective point of full condensation within the condenser (this is, approximately, the mean rate of latent heat release $(\bar{M}_{in} * h_{fg})$). For a fully condensing flow, the overall heat removal rate is, however, the sum of the latent heat released and the heat removed to sub-cool the mean exit liquid temperature below the saturation temperature.

To test whether or not the effects observed are due to the concurrent use of the pulsator and the compressor, experiments are repeated in which the pulsator is switched off and the compressor is on (in an attempt to change the mean inlet pressure at the fixed exit pressure) and, again, where the compressor is switched off and the pulsator is on (to provide different amplitudes and frequencies of the imposed pressure pulsations).

3 Results

3.1 No-Fluctuation Steady / Quasi-steady Condensing Flow Results

As depicted in Figs. 3 - 5, over the time intervals $t_1 \leq t \leq t_1^*$ and $t_3 \leq t \leq t_3^*$, the procedure described in section 2.4.1 is effective in repeatedly achieving a no - fluctuation (N-F) quasi-steady natural flow with $\bar{M}_{in} \approx 1.25$ g/s and specification of steady cooling (section 2.3) that results in steady wall temperature distributions $T_w(x)\mid_{N-F-1} \approx T_w(x)\mid_{N-F-2}$ shown in Fig. 3b. The fact that wall temperatures are only approximately recovered is partly because thermal transients take a long time to decay and partly because mean steady conditions observed in these experiments are only approximately constant. For achieving these flows, the compressor and pulsator were off, and the approximately steady-in-the-mean exit pressure was set at $p^*_{exit} = 140\ kPa$. The resulting flow has an effective point of full condensation near the exit and has a flow morphology that changes (with distance from the inlet) from wavy annular to slug / plug to bubbly to all liquid regimes (see the schematic in Fig. 1a and the photographs in Fig. 6). In Fig. 5, we see that the annular regime's rise in pressure $\Delta\bar{p}_{40cm}\mid_{N-F} = \bar{p}_{40cm}\mid_{N-F}$ - $\bar{p}_{in}\mid_{N-F} \approx 232Pa$, as measured by DPT-Test Section (see Fig. 1a) is small and heat-flux in the annular region at HFX-1 location (see Fig. 1b) is $q''_{W|N-F} \approx 0.48$ W/cm^2.

3.2 Quasi-Steady Condensing Flow with Imposed Fluctuations

In the presence of a steady pulsator driving frequency, following the procedure described in section 2.4.2, as the compressor rpm is brought from zero to a new steady value of 855 rpm (57 Hz vane frequency) and the pulsator rpm is brought from zero to a new steady value of approximately 588 rpm (9.8 Hz diaphragm frequency), a new quasi-steady condensing flow case is achieved (termed imposed - fluctuation, I-F) which is fundamentally different from the original flow in the absence of inlet pressure fluctuations. As depicted in Fig. 5, over the time intervals $t_2 \leq t \leq t_2^*$, the procedure described in section 2.4.2 is effective in achieving an altogether different quasi-steady flow with the same mean $\bar{M}_{in} \approx 1.25$ g/s and the same steady cooling (section 2.3) conditions. Over $t_2 \leq t \leq t_2^*$, the dynamic characteristics of pressure fluctuations and mass flow rate in Fig. 3 are aliased / deceptive because the data acquisition rate used to generate Fig. 5 is approximately 1 Hz. The true nature of the signals is revealed in Fig. 7 through higher speed (2000 Hz) data acquisition and a specially designed orifice plate meter whose dynamic pressure difference $(\Delta p_{om}(t))$ data are processed with the help of a special CFD technique. This is needed because the coriolis mass flow meter F_C cannot resolve the dynamic nature of the mass flow rate above 2 Hz. The larger impact on mass flow rate supports the fact that the relative amplitude of pressure - difference pulsations $\Delta p_{40cm}(t)_{IF}$ with respect to $\bar{p}_{in}$ is small, it is its relative amplitude with respect to $\Delta p_{40cm}(t)_{NF}$ is large and is what matters.

As a result of the procedure in 2.4.2, following thermal transients, a different steady wall temperature distribution $T_w(x)\mid_{I-F} \neq T_w(x)\mid_{N-F-1}$ is achieved and this is shown in Fig. 4. While achieving this new quasi-steady flow, the exit pressure control maintained $p^*_{exit} = 140\ kPa$. This new flow had a somewhat shortened length of annular flow regime, and the effective point of full condensation shifted upstream. This resulting impact on flow morphology, with respect to the schematic in Fig. 1a, changes x_A = 55 cm for the original no - fluctuation (natural, see section 2.4.1) case to x_A = 52 cm for the fluctuation induced case . For brevity, only representative photographs of the flow morphology for one of the no-fluctuation cases are shown here in Fig. 6. A more comprehensive set of photographs and discussions of flow-physics that impacts the lengths of the annular and non-annular zones is discussed in Kivisalu et al. 2011. The morphology changes between the videos associated with the no-fluctuation and imposed-fluctuation flow cases are quite noticeable and significant. The resulting changed values of the mean pressure rise $\Delta\bar{p}_{40cm}\mid_{I-F} \approx 362\ Pa$ and mean heat flux $\bar{q}''_{W|I-F} \approx 2.06$ W/cm^2 at the HFX-1 location in Fig.

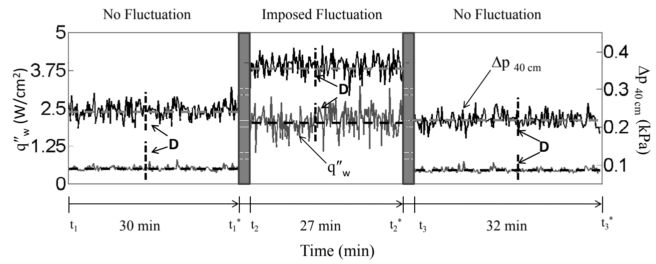

Fig. 3 Inlet mass flow rate, and inlet to exit pressure difference for no-fluctuation and imposed-fluctuation flow cases.

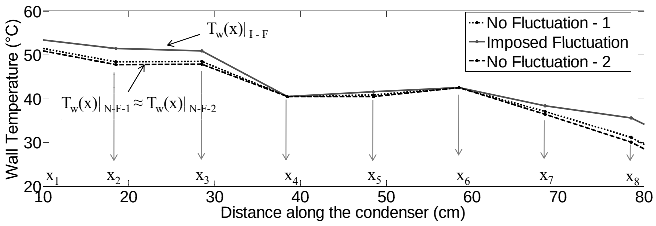

Fig. 4 Steady wall temperature distributions for no-fluctuation and imposed-fluctuation flow cases

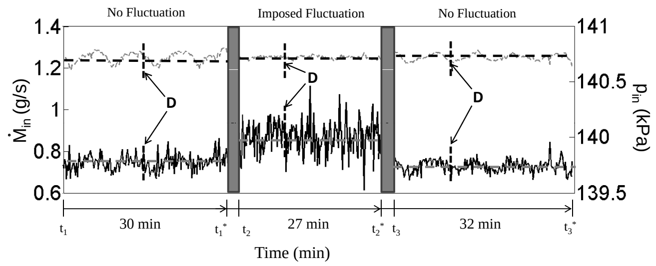

Fig. 5 Heat flux (HFX-1) and test section differential pressure (DPT-Test Section) reading Δp_{40cm} for no-fluctuation and imposed-fluctuation cases (see Fig. 1 for sensor locations)

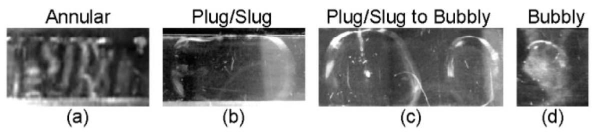

Fig. 6 Liquid-vapor interface for natural (N-F) flow at locations represented by x_a, x_b, x_c, and x_d in Fig. 1a

1b (an increase of approximately 329% over the original no-fluctuation case value) are shown in Fig. 5.

For the fully condensing flows at approximately the same total heat load, the above reported multiple quasi-steady flow realizations lead to: significant redistribution of wall heat flux, changes in condensing-surface temperatures, change from essentially quasi-steady non-annular regimes for the original no - fluctuation case to oscillating non - annular regimes for the fluctuation induced case (observed in the video for the cases with inlet pressure fluctuations), etc.

3.3 Role of Fluctuations in Attaining Different Quasi-Steady Flows

To better understand the role of amplitude and frequency content of fluctuations on attaining different steady-in-the mean flows, we look at *5 s long* dynamic signals (acquired at DAQ rate of 2000 Hz) for: inlet pressure, exit pressure, heat flux at HFX-1 location ($q''_w(t)\ |_{HFX-1}$, see Fig. 1b), and test-section pressure difference $\Delta p\ |_{40cm}$. These dynamic signals are obtained at certain times (labeled D in the time-histories of these variables shown in Figs. 3, 5). The time domain dynamic signals of $\Delta p_{om}(t)$ and $\dot{M}_{in}(t)$ are shown in Fig. 7. The frequency domain plots (obtained by Fast Fourier Transforms, FFTs) of $[p'_{in}(t) \equiv p_{in}(t) - \bar{p}_{in}]$, $[q''_w(t)\ |_{HFX-1}]$, $[p'_{exit}(t) \equiv p_{exit}(t) - \bar{p}_{exit}]$, $[\Delta p_{40cm}(t)]$ and $[\dot{M}_{in}(t)]$ are respectively shown in Figs. 8-12. It is clear from Fig. 8 that the pulsator-induced frequencies (9.8 Hz and its harmonics) are present for the imposed-fluctuation case but not for the no-fluctuation imposed cases. It was experimentally verified (not reported here) that: (a) the same pulsations from the pulsator with the compressor kept off, again had a similar and significant impact on the flow (see Kivisalu et al. 2011), and, (b) with or without the pulsator fluctuations, an increase in the compressor speed or partial closing of V_{BP} did not noticably influence the pressure difference across the condenser. It is known from other considerations for unsteady partially condensing flows (as discussed in Kulkarni et al. 2011 and Kivisalu et al. 2011) that fluctuations (or other type of unsteadiness) are necessary to deviate from the *natural* no-fluctuation quasi-steady flows. Also, Kivisalu et al. 2011 discusses how the time averaged values of the high amplitude fluactuation I-F quasi-steady case can be considered to be arising from elliptic sensitivity. This is due to the fact that averaging takes place over large time scales that involve both forward and backward moving interfacial waves. A demonstration of analogous fluctuation-sensitivity for partially condensing annular flows (analogous to the upstream annular portion of the reported fully condensing flows) requires additional experiments and will be reported in subsequent papers. The increase in heat-flux at the HFX-1 location of Fig. 1b, as shown in Fig. 5 and Fig. 9, is made possible by a significant reduction in the mean condensate thickness at that location. This is perhaps due to the nature of mass flow rate fluctuations (Fig. 7) over its mean that is achieved by the alternately forward and backward moving interfacial waves. During this time, condensate maintains a mean forward motion and waves are able to reflect at end of the annular regime because the requisite physical conditions for wave reflection exist and / or can be arranged to exist. It is conjectured (and is being computationally established) that, over a representative period of fluctuation, the decreasing film thickness behavior associated with the larger amplitude positive mass flow rate fluctuation over its mean domi-

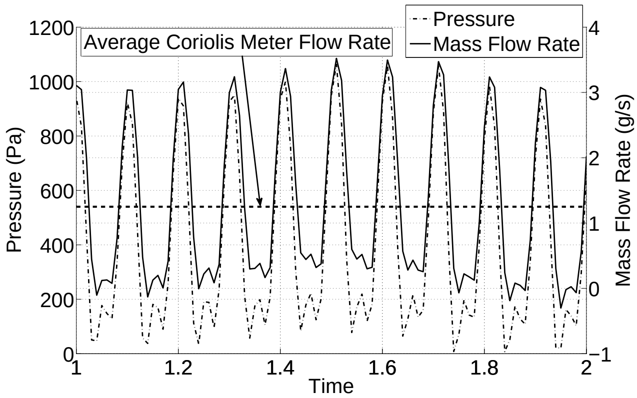

Fig. 7 Orifice plate pressure difference signal $\Delta p_{om}(t)$ and associated mass flow rate signal $\dot{M}_{in}(t)$.

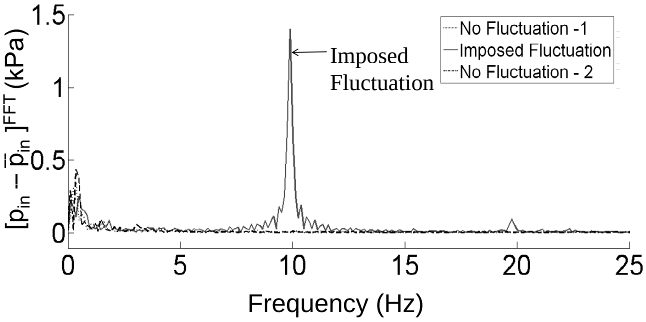

Fig. 8 FFTs of $[p'_{in}(t)\ ]$ for no-fluctuation and imposed-fluctuation flow cases.

nates the increasing film thickness behavior associated with the lower amplitude and longer duration negative mass flow rate fluctuation. As expected, this thickness (which is, approximately, inversely proportional the local heat-flux) still oscillates around its mean location with the same predominant frequencies that are present in the pressure-difference or the mass-flow rate fluctuations. The frequency content of the inlet mass flow rate fluctuations in Fig.7, as obtained by the FFT of $[\dot{M}_{in}(t)]$, is shown in Fig. 12. At 9.8 Hz and its harmonics, the reduced amplitude of exit pressure fluctuations (Fig. 10) relative to the inlet pressure fluctuations (Fig. 8) clearly indicates the condensing flows' ability to absorb these fluctuations so as to change the mean quasi-steady characteristics of the flow. These fluctuations in the pressure- difference between the inlet and the exit of the condenser couple with the mass flow rate fluctuations in the incoming vapor to induce significant changes ($> 500\%$) in both the mean and fluctuating mechanical energy that is consumed (expression on the left side of Eq. (A.11) of Kulkarni et al. 2011) within the test-section.

For brevity, this paper only deals with the reported impact of inlet pressure and flow fluctuations at one frequency setting of the pulsator. This case is representative of many such cases discussed and termed super-critical fluctuations

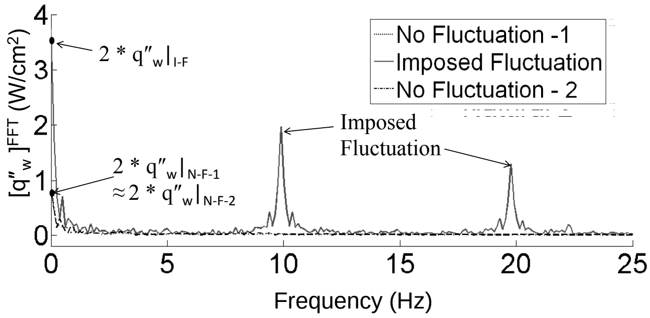

Fig. 9 FFTs of $[q''_w(t)_{HFX-1}\ ]$ for no-fluctuation and imposed-fluctuation flow cases.

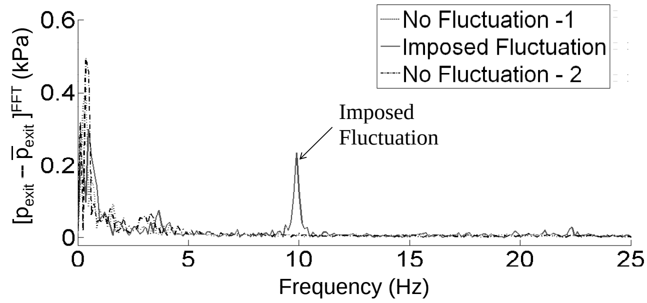

Fig. 10 FFTs of $[p'_{exit}(t)\ ]$ for no-fluctuation and imposed-fluctuation flow cases

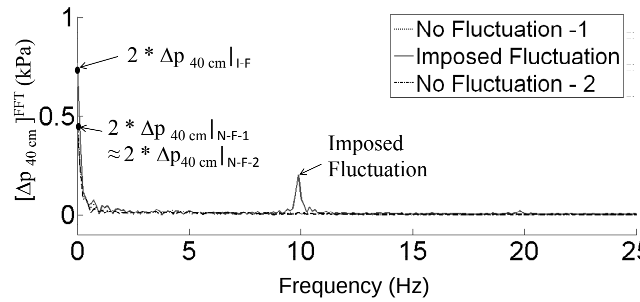

Fig. 11 FFTs of $[\Delta p_{40cm}(t)]$ for no-fluctuation and imposed-fluctuation flow cases.

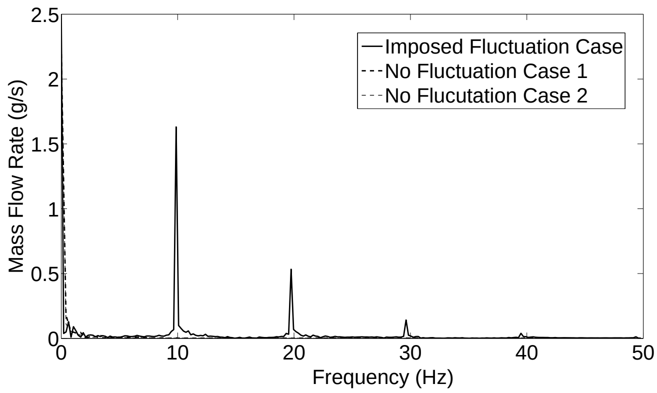

Fig. 12 FFTs of $[\dot{M}_{in}(t)]$ for no-fluctuation and imposed-fluctuation flow cases.

in Kivisalu et al. 2011. The no-imposed fluctuation case is physically characterized by FC-72 properties, the channel geometry (gap h = 2 mm), and the conditions: $\bar{p}_{in}$ =139.7kPa , $\dot{M}_{in} = 1.25 g/s$ (average inlet vapor speed U = 2.32 m/s), representative inlet saturation temperature T_{sat} of = 66.33^{o}C, mean condensing - surface temperature $\bar{T}_w$ = 50.8^{o}C and an associated non - dimensional temperature variation profile. The non - dimensional numbers characterizing these conditions are defined in Mitra et al. 2011 (and their values are $Re_{in} = 7682$, $Ja = 0.216$, $Pr_1 = 8.2$, $\rho_2/\rho_1 = 0.011$, $\mu_2/\mu_1 = 0.021$, $0 \leq x/h \leq x_A/h$ where $x_A/h \approx 275$). For the imposed fluctuation case, in addition to the non-dimensional numbers reported above, non-dimensional values of the imposed frequency f (Strouhal number $St = f * h/U = 0.0085$) and the amplitude of the imposed pressure - difference fluctuation (defined as the ratio of the FFT amplitude of $[\Delta p_{40cm}(t)\ |_{I-F}]$ at $f = 9.8 Hz$ and the mean value of $[\Delta p_{40cm}(t)\ |_{N-F}]$ is, in this case, about 1.5625) are needed. A range of these numbers associated with the larger data set investigated in Kivisalu et al. 2011 can be similarly calculated and is being reported in a separate paper.

4 Conclusions

The reported experimental results demonstrate that significantly different quasi-steady pressure difference realizations across a shear / pressure driven condenser (as in horizontal, zero-gravity and micro-scale applications) are achieved if suitable (but typical) fluctuations are present on a steady-in-the-mean inlet pressure and flow rate. This leads to significantly different quasi-steady flow realizations for the same quasi-steady mass flow rate, exit pressure and cooling conditions. If the resulting effects on flow morphology, local heat transfer rates, and associated significant thermal transients are not taken into account, they may lead engineers to believe that the condenser performance is either non-repeatable or non-deterministic.

The above results are consistent with the fact that, under no-fluctuation conditions for a given mean inlet vapor flow rate and steady cooling condition, the condenser exhibits only one unique natural quasi-steady flow and associated self-sought pressure difference.

Acknowledgements This work was supported by NASA Grant NNX-10AJ59G and NSF Grant CBET-1033591.

References

1. Ajotikar, N., Dynamic gas flow rate measurements based on a mixed computational - experimental approach for processing dynamic pressure - difference signals obtained across a specially designed orifice-plate meter, Master of Science Thesis, Michigan Technological University (2011)
2. Brutin, D., Topin, F., Tadarist, L, Experimental study of unsteady convective boiling in heated minichannels. Int. J. Heat and Mass Transfer 46, 2957-2965 (2003)
3. Cavallini, A., Smith, J.R., Zechchin, R, A Dimensionless Correlation for Heat Transfer in Forced Convection Condensation. 6th Int. Heat Transfer Conference, Tokyo, Japan (1974)
4. Cavallini, A., Zechchin, R, High velocity condensation of R-11 vapors inside vertical tubes. Heat Transfer in Refrig., 385-396 (1971)
5. Coleman, J.W., Garimella, S, Two-phase Flow Regimes in Round, Square, and Rectangular Tubes during Condensation of Refrigerant R134a, Int. J. Refrig. 26, 117-128 (2003)
6. Goodykoontz, J.H., Dorsch, R.G., Local heat transfer coefficients for condensation of steam vertical down flow within a 5/8-inch diameter tube. NASA TN D-3326 (1966)
7. Kandlikar, S. G. Fundamental issues related to flow boiling in minichannels and microchannels. Experimental Thermal and Fluid Science, 26, 2-4, 389-407 (2002)
8. Kivisalu, M., Gorgitrattanagul, N., Mitra, S., Naik, R., and Narain, A., Shear / r Pressure Driven Internal Condensing Flows and their Sensitivity to Inlet Pressure Fluctuations, Paper Number IMECE2011-63281, Proceedings of ASME International Mechanical Engineering Congress and Exposition, Denver, Colorado, USA (2011)
9. Kulkarni, S. D., Narain, A., Mitra, S., Kurita, J. H., Kivisalu, M., Hasan, M. M, Flow Control and Heat Transfer Enhancement in Presence of Elliptic-Sensitivity for Shear Driven Annular/Stratified Internal Condensing Flows. in press for publication in Int. J. of Transport Phenomena (2011) Draft available at: http://www.me.mtu.edu/ narain
10. Kurita, J. H., Kivisalu, M., Mitra, S., Narain, A., Experimental Results on Partial and Fully Condensing Flows in Vertical Tubes, Their Agreement with Theory, and Results on Exit-Condition Sensitivity, Int. J. of Heat and Mass Transfer 54, 2932-2951 (2011)
11. Mitra, S., Narain, A., Naik, R., Kulkarni, S. D., A Quasi One-Dimensional Method and Results for Steady Annular/Stratified Shear and Gravity Driven Condensing Flows. in press for publication in Int. J. of Heat and Mass Transfer 54, 3761-3776 (2011)
12. Narain, A., Q. Liang, G. Yu, X. Wang, Direct Computational Simulations for Internal Condensing Flows and Results on Attainability/Stability of Steady Solutions, Their Intrinsic Waviness, and Their Noise-Sensitivity, Journal of Applied Mechanics (71), pp. 69-88 (2004)
13. Shah, M.M., A General Correlation for Heat Transfer during Film Condensation inside Pipes. Int. J. of Heat and Mass Transfer 22, 547-556 (1979)
14. Wedekind, G.L., Bhatt, B.L., An Experimental and Theoretical Investigation in to Thermally Governed Transient Flow Surges in Two-Phase Condensing Flow. ASME Journal of Heat Transfer 99, 4, 561-567 (1977)
15. Wu, H.Y., Cheng, P., Condensation Flow Patterns in Microchannels. Int. J. Heat and Mass Transfer 48, 286-297 (2005)